nature communications

Article

https://doi.org/10.1038/s41467-024-52341-2

Optically accessible long-lived electronic biexcitons at room temperature in strongly coupled H- aggregates

Received: 28 November 2023

Accepted: 2 September 2024

Published online: 27 September 2024

Check for updates

Siddhartha Sohoni[1,2,3,4,5], Indranil Ghosh[1,2,3,4,5], Geoffrey T. Nash[1], Claire A. Jones[1,2,3,4], Lawson T. Lloyd[1,2,3,4], Beiye C. Li[1,2,3,4], Karen L. Ji[1,2,3], Zitong Wang[1], Wenbin Lin[1] & Gregory S. Engel[1,2,3,4]

Photon absorption is the first process in light harvesting. Upon absorption, the photon redistributes electrons in the materials to create a Coulombically bound electron-hole pair called an exciton. The exciton subsequently separates into free charges to conclude light harvesting. When two excitons are in each other's proximity, they can interact and undergo a two-particle process called exciton-exciton annihilation. In this process, one electron-hole pair spontaneously recombines: its energy is lost and cannot be harnessed for applications. In this work, we demonstrate the creation of two long-lived excitons on the same chromophore site (biexcitons) at room temperature in a strongly coupled H-aggregated zinc phthalocyanine material. We show that exciton-exciton annihilation is suppressed in these H- aggregated chromophores at fluences many orders of magnitudes higher than solar light. When we chemically connect the same aggregated chromophores to allow exciton diffusion, we observe that exciton-exciton annihilation is switched on. Our findings demonstrate a chemical strategy, to toggle on and off the exciton-exciton annihilation process that limits the dynamic range of photovoltaic devices.

Electronic excitations created in materials upon photoexcitation delocalize over several aggregated molecules when the electrostatic coupling between them is strong[1–3]. Delocalization changes the photophysical properties of the aggregate relative to the single chromophore and can alleviate trapping processes that halt exciton diffusion[4]: energetic relaxation[5] and excimer formation[6]. However, it also facilitates exciton-exciton annihilation[7–11], a process that limits the dynamic range and efficiency of light-harvesting at high photon fluence. Chromophores are said to be strongly coupled to one another when the coupling energy is much larger than the energies of active vibrational modes of the chromophores[12,13].

Positive electrostatic coupling between chromophores results in a blueshift of the absorption spectrum of the aggregate from the constituent monomer's absorption. Positively coupled aggregates are commonly referred to as H- aggregates[12]. Upon positive coupling, the highest-energy eigenstate of the aggregate is optically bright and the lowest-energy state is optically dark. This lowest-energy state in H- aggregates is dark because its spatial wavefunction is highly oscillatory, with adjacent monomers in the aggregate having alternating positive and negative wavefunction coefficients. The oscillatory wavefunction of the lowest-energy excited-state makes the transition to it from the electronic ground-state forbidden by selection rules[12].

Exciton-exciton annihilation (EEA) can occur when two excitons collide. It reduces the efficiency of light harvesting at high fluences. EEA is a second-order kinetic effect because it is dependent on

[1]Department of Chemistry, The University of Chicago, Chicago, IL, USA. [2]The Institute for Biophysical Dynamics, The University of Chicago, Chicago, IL, USA. [3]James Franck Institute, The University of Chicago, Chicago, IL, USA. [4]Pritzker School for Molecular Engineering, The University of Chicago, Chicago, IL, USA. [5]These authors contributed equally: Siddhartha Sohoni, Indranil Ghosh. e-mail: gsengel@uchicago.edu

two-particle collisions[14], and it results in one exciton decaying to the ground state non-radiatively, thereby lowering the quantum yield of the photovoltaic process. Circumventing EEA could be a possible design route towards increasing the dynamic range in photovoltaics and other optoelectronics.

EEA is routinely probed with fluence-dependent third-order nonlinear spectroscopy[1,7–10,14–17]. Two interactions between an exciting pulsed electric field and the material create exciton populations. These populations are then probed with a third field interaction in third-order nonlinear spectroscopy. Upon increasing the fluence of the exciting pulses, the likelihood of fifth-order interactions increases because more excitons are created in the same excitation volume increasing the cross-section of exciton-exciton collisions. At high fluences, exciton dynamics often show a distinct second-order population decay that arises from exciton-exciton collisions leading to annihilation. In nonlinear spectroscopy, a second order effect results from four interactions with the exciting electric field as opposed to two interactions. The likelihood of four interactions increases with increasing pump fluence because more excited-state particles are created within the same sample.

Recently, Tempelaar and coworkers and Huang and coworkers showed theoretically and experimentally that the oscillatory property of H- aggregate wavefunctions could be used to suppress EEA[16,18]. The EEA rate was shown to be proportional to the square of the sum of wavefunction coefficients along the sites of aggregates by Tempelaar and coworkers[18]. Exciton lifetime was also shown to increase with fluence in Cy5 H-aggregates[19]. Coherent suppression of exciton-exciton annihilation is attributed to oscillatory spatial wavefunctions in H-aggregate bands that make the sum of wavefunction coefficients over all chromophores vanishingly small in the strong-coupling limit[18]. The oscillatory character of the wavefunctions makes interactions between different excitons small, suppressing the manifestation of this multiparticle effect in H- aggregates[16]. Huang and coworkers found however that EEA occurs at room temperatures in H- aggregates because exciton diffusion allows collisions between excitons of many different spatial phases[16]. At low temperature however, they observed that EEA was strongly suppressed because exciton diffusion slowed down[16]. Coherent suppression of EEA could be utilized to enhance the light-harvesting capabilities of photovoltaics.

In this work, we compare exciton dynamics in single and chemically connected H- aggregates at room temperature. We find that the biexciton state can be accessed instantaneously in both single and connected aggregates within 10 femtoseconds. However, exciton-exciton annihilation is suppressed between the excitons created on single H- aggregates.

To form our H-aggregates, we use zinc(II)−2,3,9,10,16,17,23,24-octa(4-carboxyphenyl)phthalocyanine, ZnOPPc[20,21] which has eight hydrogen bonding arms (Fig. 1a). In DMSO, ZnOPPc is stabilized in its monomeric state with a strong Q-band at 710 nm with prominent blue vibronic shoulders. π-stacking is dominant in aqueous environments and results in strongly coupled, H-aggregated chromophores with an absorption maximum at 650 nm (Fig. 1c). At pH 11 in aqueous medium, the phthalocyanine carboxylate arms are deprotonated. Deprotonation results in repulsion between aggregates so that individual, disconnected aggregates are dispersed in solution. At neutral pH, the aggregates become protonated and hydrogen-bond to one another to self-assemble into a crystalline hydrogen-bonded organic framework of H-aggregates (HOF) (Figs. 1b, d).

We perform fluence-dependent pump-probe spectroscopy on the dispersed aggregates and HOF. With isolated aggregates, we observe a quadratic dependence of signal intensity with fluence, but no annihilation. In the HOF, we observe sub-5 ps exciton-exciton annihilation, consistent with previous reports on phthalocyanine-based aggregates[22,23]. These results show that exciton-exciton annihilation occurs due to excitonic motion along the hydrogen bonding direction. However, annihilation can be eliminated if exciton transfer between aggregates is prevented. Biexcitons exist on individual aggregates dispersed in solution without annihilating. We perform two-dimensional electronic spectroscopy on dispersed aggregates and frameworks to observe the instantaneous formation of a minimally redshifted[24,25] biexciton state. Cross-peak specific two-dimensional electronic spectroscopy reveals orthogonal valleys in the H-aggregate band structure, possibly arising from the two near-degenerate, orthogonal, Q-transitions. Our observations provide a mechanism for the observed temperature-dependence of EEA[16] and a chemical route to greatly increase the dynamic range of light-harvesting antennae.

Results

Design and structure of single and connected ZnOPPc aggregates

The molecular structure of monomeric ZnOPPc, linear absorption spectra of the monomer, single H-aggregates, and HOF, and images of self-assembled HOF are shown in Fig. 1. The chemical structure of ZnOPPc is shown in Fig. 1a. Synthesis of ZnOPPc has been reported previously[20,21] and is summarized in Supplementary Notes Section 1. In aprotic solvents such as dimethyl sulphoxide (DMSO) and N, N – dimethyl formamide (DMF), ZnOPPc maintains its monomeric structure and does not form hydrogen bonds or π-stacks, showing a strong Q band absorption at ~710 nm. In water at neutral pH, π-stacked-aggregates self-assemble via hydrogen bonding to form a crystalline H-aggregated, hydrogen-bonded organic framework (HOF). Aggregation of phthalocyanine and naphthalocyanine moieties in water to form H-aggregates has been reported in the past[22,23,26,27]. ZnOPPc's hydrogen bonding through eight peripheral carboxylic acid groups allows the formation of an ordered and long-range crystalline framework as opposed to an amorphous aggregate[22,23,26]. Figure 1b, d show transmission electron microscopy (TEM) and atomic force microscopy (AFM) images of HOFs of connected aggregates. Rod-like framework structures, ~35 nm in diameter and > 200 nm in length are formed in contrast to tubular porphyrin J-aggregate structures reported earlier[28]. Dynamic light scattering (DLS) and X-ray diffraction (XRD) measurements of the HOF are shown in the Supplementary Figs. 8, 9. The HOF suspension remains colloidally stable over the course of characterization and spectroscopy for several weeks. ZnOPPc is weakly fluorescent as a monomer[21] and its fluorescence is further suppressed in the framework to nearly undetectable levels, which blocks the radiative recombination pathway for excitons. From the high-resolution TEM image and XRD pattern, a lattice spacing of ~2 nm is obtained, suggesting that π-stacking occurs along the length of the framework and hydrogen bonding along the other two dimensions. The pH of this aqueous framework of aggregates with minimal DMSO used for initial dissolution of the monomer was measured to be 7.1. In contrast, when the monomer is dissolved in aqueous NaOH to make a final pH of 11.7, connected aggregates do not form, and no ordered structures are seen in TEM images. However, the absorption spectra of basic and neutral solutions of ZnOPPc are nearly identical, confirming that π-stacking (which leads to the spectral blueshift) and HOF self-assembly are along orthogonal directions. This observation also suggests that H-interactions in phthalocyanines are mainly due to face-to-face stacking interactions. TEM images of the basic solution are shown in the Supplementary Notes Section 1.3 and show no crystalline domains. We calculate the degree of coupling in the aggregates using the nearest-neighbor approximation[3] to be $V_O \approx +1000\ cm^{-1}$ which is much larger than the static disorder seen in the monomer from the difference between the diagonal and antidiagonal linewidths of the monomer 2D spectra (Supplementary Fig. 24)[29]. The coupling is calculated as the difference between the aggregate and monomer absorption maxima as prescribed by Hestand and Spano[12].

https://doi.org/10.1038/s41467-024-52341-2

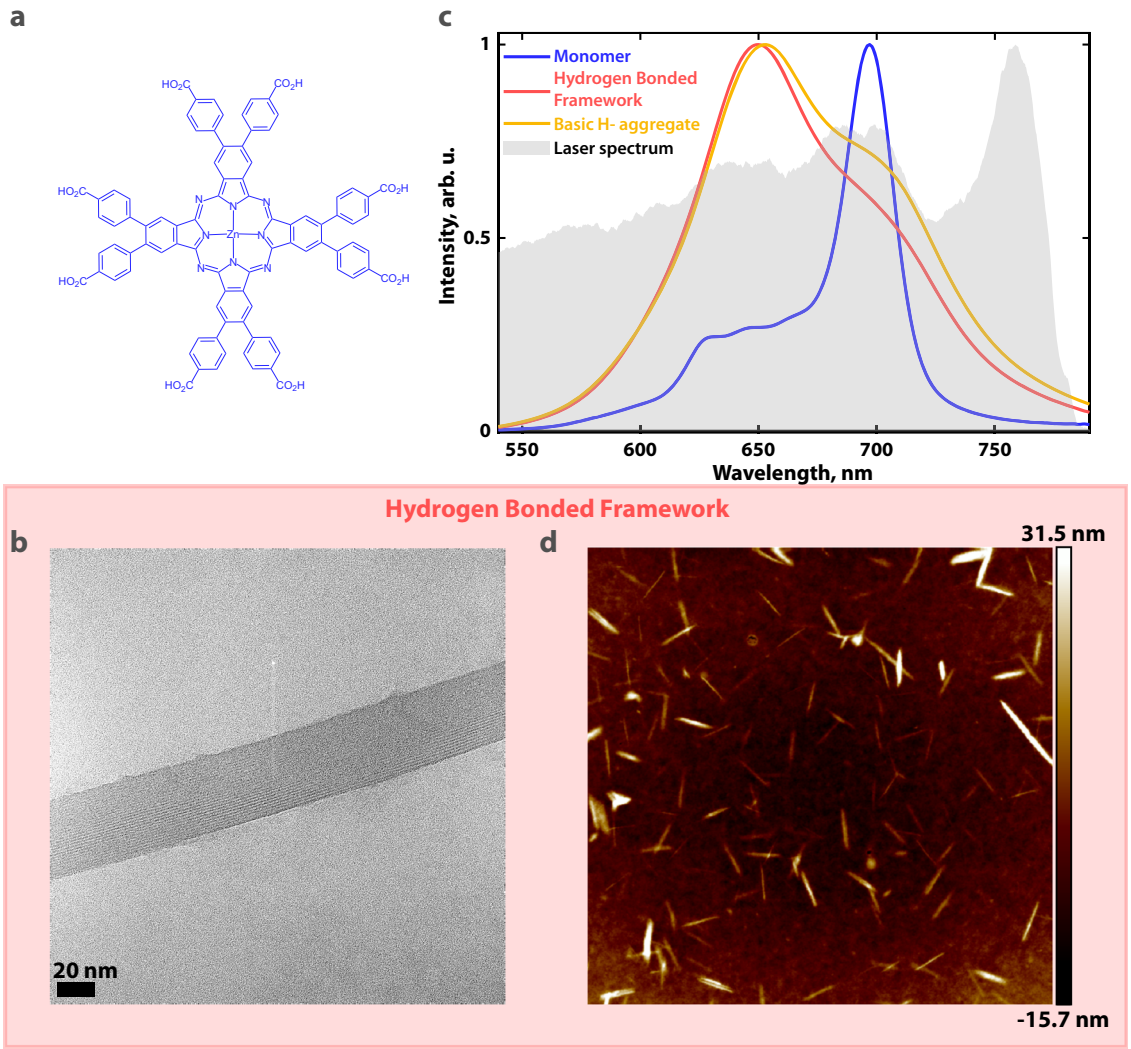

Fig. 1 | Structure of Zinc Phthalocyanine H- aggregates. a Structure of zinc(II) −2,3,9,10,16,17,23,24-octa(4-carboxyphenyl)phthalocyanine (ZnOPPc) (**b**) Transmission electron microscopy (TEM) images of the framework of aggregates, scale bar is 20 nm (**c**) Absorption spectra of ZnOPPc monomer (in DMSO), H-aggregate (in aq. NaOH) and HOF (connected aggregates, in neutral H_2O) with the laser spectrum used for two-dimensional electronic spectroscopy (2DES) and fluence-dependent pump-probe experiments (**d**) Atomic force microscopy (AFM) profile distributions for several HOF particles, scale bar is 1 micron. Source data are provided as a source data file.

Two-dimensional Electronic Spectroscopy and Electronic Structure of Single and Isolated Aggregates

We performed two-dimensional electronic spectroscopy (2DES) on dispersed and connected H-aggregates. Two-dimensional electronic spectroscopy provides time-resolved excitation and detection energy information of the electronic structure of materials. Positive features in 2DES spectra arise from ground state bleach (GSB) and stimulated emission (SE) Feynman pathways. Negative features in 2DES spectra arise from photoinduced/pump-induced absorption (PIA). Excited-state absorption of pump-excited chromophores and ground-state absorption of chromophores coupled to excited chromophores creates PIA signals in 2DES spectra. 2DES spectra of single and connected aggregates at 20 fs are shown in Fig. 2 along with the time-evolution of the two main peaks that we observe. 2DES is performed with ~6 fs pulses and a ~ 9 fs instrument response function (see Suppl. Notes Section 2). The laser spectrum is shown in Fig. 1b.

2DES spectra of both single aggregates and HOF show qualitatively similar features with derivative lineshapes characteristic of biexcitons in strongly coupled systems[30–33] (Figs. 2b, c). The broad PIA feature seen above the diagonal is replicated in both systems and appears at earliest times with no discernable time-constant associated with its growth. We attribute this feature to the direct optical formation of a biexciton ($|ee\rangle$) state. When excitons share a common ground state, excitation into the two-exciton manifold creates a biexciton state of two coupled excitons, which we depict as $|ee\rangle$ in the Feynman pathway in Fig. 2f, and as an energy-level diagram in Fig. 2e. This state is different from a state with two non-interacting excitons that are not Coulombically coupled to each other, and from excitation into a higher energy level/band from the conduction band. The ground-state coupling of the two excitons of the biexcitonic state yields a photoinduced absorption feature in 2DES, yielding a dispersive lineshape along the detection axis[30,34]. In other materials, like monolayer MoS_2, biexciton features do not appear in third order experiments until the system has evolved for about 50 fs following direct excitation precluding direct optical excitation of biexcitons with a single short (6 fs) laser pulse[32]. We can rule out the formation of a charge-separated state or excimer[6,35] in both isolated and connected aggregates because the photoinduced absorption feature does not change up to 100 ps in pump-probe spectra (Supplementary Fig. 26). Moreover, we do not observe broad excimer fluorescence from either single or connected aggregates. We also conclude that relaxation from the bright, highest-energy state to the dark state is rapid because no significant spectral

https://doi.org/10.1038/s41467-024-52341-2

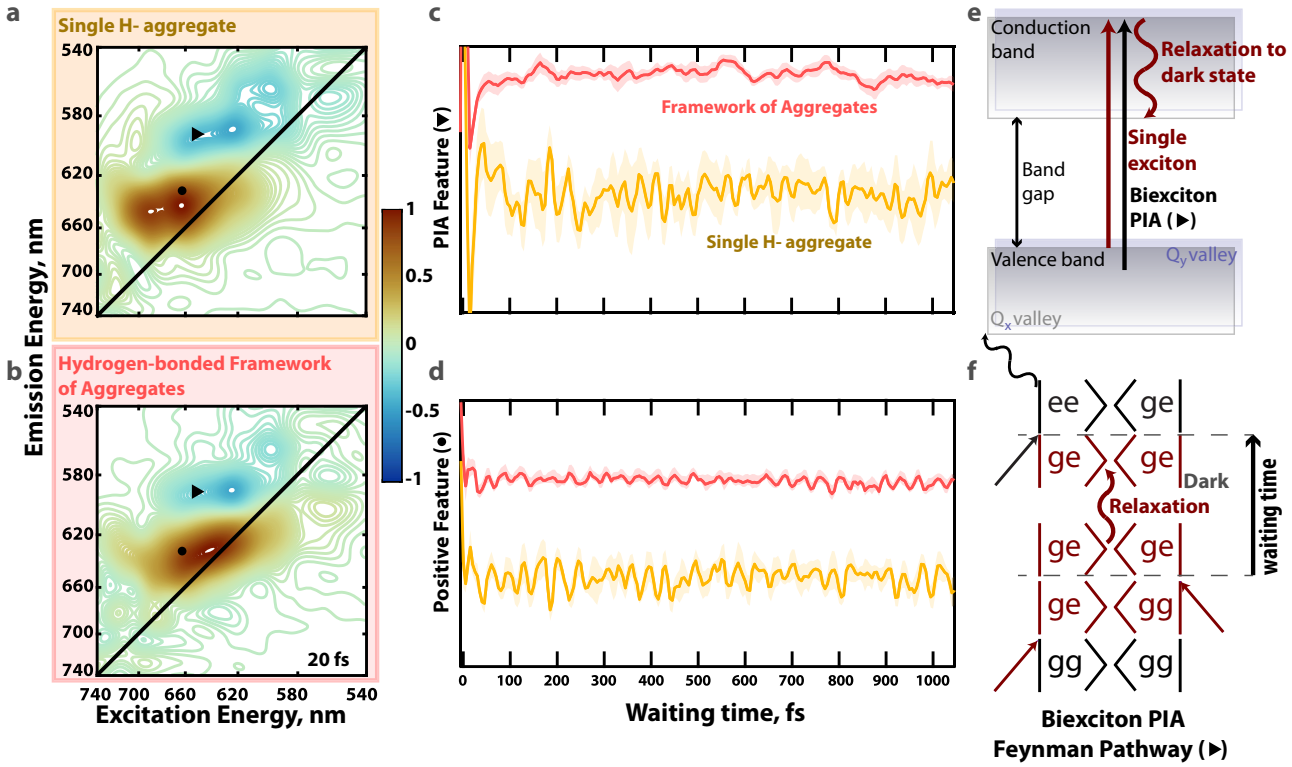

Fig. 2 | Phased Two-dimensional Electronic Spectra of Single and Connected Aggregates. Representative absorptive 2DES spectra of (**a**) isolated ZnOPPc aggregates (average of $n = 5$ spectra) and (**b**) HOF at 20 fs (average of $n = 10$ spectra). (**c**) normalized and offset photoinduced absorption (shaded error bars are 1 standard error in the mean) and (**d**) ground-state bleach feature time traces from 2DES data from the marked points in **a** and **b** (shaded error bars are 1 standard error in the mean). Pump, probe and local-oscillator polarizations are kept parallel to each other when collecting this data. In **a**, **b**, **c**, and **d**, • is located at excitation wavelength = 660 nm and detection wavelength = 630 nm and represents ground state bleaching dynamics. ▼ represents the photoinduced absorption feature at excitation wavelength = 650 nm and detection wavelength = 595 nm. Source data for a, b, c, and d are provided as a Source Data file. **e** Energy-level diagram of the aggregate bands to depict biexciton formation and the negative PIA feature observed in both aggregates in **a** and **b**. The corresponding biexciton ($|ee\rangle$) formation Feynman pathway is shown in (**f**). Pump interactions are shown in maroon. The probe interaction, or biexciton formation process, is shown in black.

evolution is seen in the PIA feature over 1 ps after the first ~50 fs. The excited-state absorption feature has a broader lineshape than the ground-state bleach and Rabi contraction[30,31,36] in this system seems to be minimal because the negative signal is not redshifted from the positive signal. Finely sampled 2DES measurements reveal that the electronic structure of the aggregate and its ultrafast excited state dynamics do not change significantly upon being connected to/disconnected from other aggregates. They also reveal that the excited-state electronic structure does not change significantly after ~50 fs from excitation, ruling out processes like excited-state absorption, excimer formation, and trapping, while strongly suggesting the formation of a biexciton upon probe interaction in both samples. Centerline slope analysis of the main ground state bleach feature of the 2DES spectra of both connected and isolated aggregates further confirms that pH change does not impact the excited-state dynamics of the system (Supplementary Fig. 23).

We perform cross-peak-specific 2DES on connected and dispersed H- aggregates to eliminate the prominent ground-state bleach feature to selectively observe the dynamics of the PIA feature. The cross-peak-specific 2DES sequence reports signals emitted from transitions with non-parallel transition dipoles[24,25,37]. Population dynamics arising from light-matter interactions governed by parallel transition dipoles is suppressed in the cross-peak specific sequence[24,37]. It is important to note that a cross-peak can appear on the main diagonal provided that the feature arises from near-degenerate states with non-parallel transition dipole moments[25,34]. Cross-peak-specific 2DES spectra of single aggregates and HOF are shown in Fig. 3.

The Q-band transitions of phthalocyanines that couple to form H-aggregate excited state bands are doubly-degenerate[38] with perpendicular dipole moments (Fig. 3g). In cross-peak-specific spectra of both samples, we see a cross-peak on the diagonal at the location of the ground-state bleach and along the observed PIA feature in all-parallel spectra (see Supplementary Fig. 22 for overlaid spectra). This peak is present from $T = 0$, and does not show any appreciable spectral evolution over the finely sampled first picosecond. The instantaneous observation of a cross-peak displaying negligible spectral evolution over delay time in both connected and single aggregates points strongly towards a ground-state coupling between non-parallel transition dipole moments within single H- aggregates. These observations suggest that the PIA feature is unlikely to be excimer formation because no spectral evolution is observed over either 1 ps or the lifetime of the aggregates (see Supplementary Fig. 26). Our cross-peak specific spectra reveal orthogonal valleys in the bands in these phthalocyanine H-aggregates. It is likely that orthogonal bands arise from coupling of the perpendicular Q- bands of individual phthalocyanine molecules.

The biexcitonic binding energy can be estimated from the difference between the emission energy of the cross-peak maximum (biexciton signature) and the linear absorption peak and is calculated to be around 400 cm^{-1}. The absence of a spectral redshift of the biexciton photoinduced absorption feature with respect to the ground-state bleach in this system suggests that the biexciton binding energy is low and the excitons are relatively noninteracting, possibly due to the highly oscillatory wavefunctions of these excitons and the orthogonality of the Q_x and Q_y valleys of the excited-state band. Other

https://doi.org/10.1038/s41467-024-52341-2

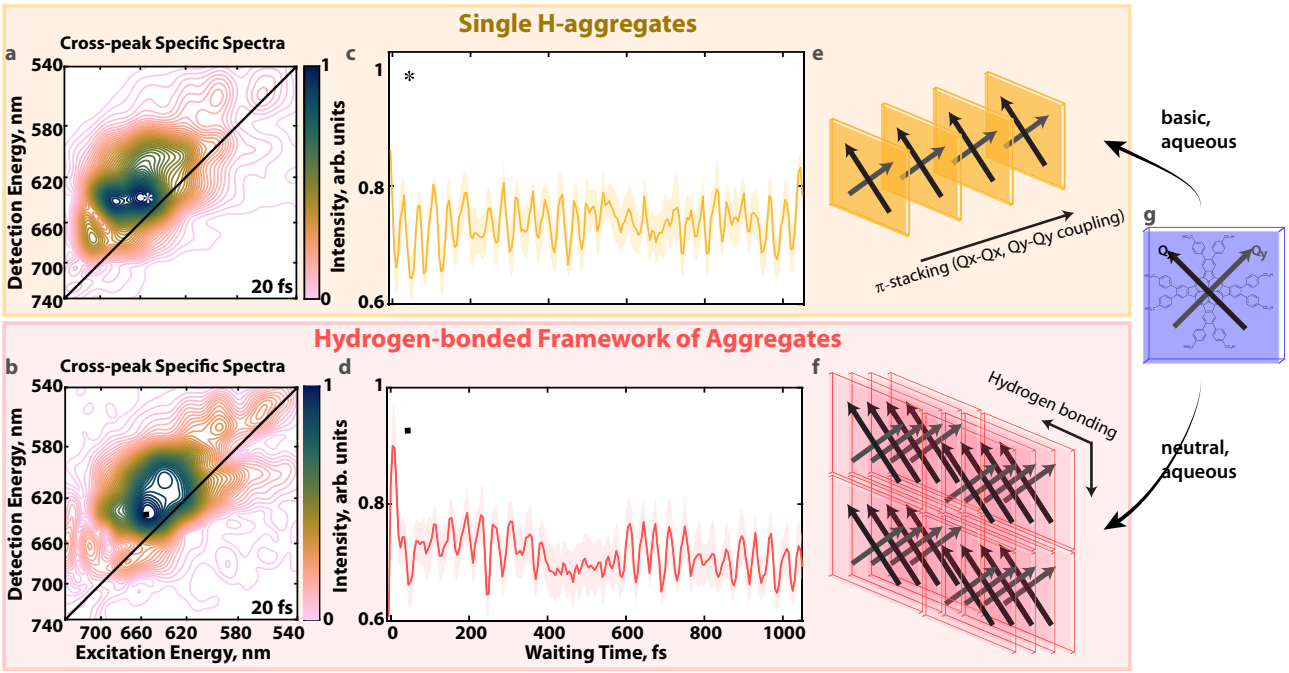

Fig. 3 | Cross-peak-specific 2DES spectra of single and connected aggregates. Cross-peak specific 2DES spectra showing the absolute value of the response in the ⟨90, 60, 120, 0⟩° polarization sequence of (**a**) single (average of $n = 7$ spectra) and (**b**) connected aggregates at 20 fs (average of $n = 6$ spectra). Time evolution of the main cross-peak across 1 ps is shown for (**c**) single (shaded error bars are 1 standard error in the mean) and (**d**) connected aggregates (shaded error bars are 1 standard error in the mean). * represents the peak position in the cross-peak specific spectrum of the isolated aggregates at excitation wavelength = 660 nm and detection wavelength = 640 nm. ■ represents the peak position in the cross-peak specific spectrum of connected aggregates at excitation wavelength = 650 nm and detection wavelength = 640 nm. Source data for a, b, c, and d are provided as a source data file. **e** and **f** show the formation of orthogonal bands upon phthalocyanine π- stacking which leads to coupling of orthogonal Q-band dipole moments. **g** shows the orthogonal Q_x and Q_y phthalocyanine dipole moments.

studies have seen convolved spectral signatures of biexcitons in H-aggregates[39,40], and directly in perovskites through two-quantum white-light microscopy[41]. We observe the ground-state coupling directly through the cross-peak specific sequence[24,25,37] and attribute it to the excitation of the two near-degenerate, perpendicular Q-bands.

Our 2DES experiments reveal an instantaneous PIA feature in both aggregate samples, which we attribute to biexciton formation upon probe interaction. 2DES allows us to observe the ultrafast formation of this manifold without the pulse overlap artifact that is a limitation in pump-probe spectroscopy. Cross-peak specific 2DES reveals that the biexciton manifold can be instantaneously accessed through non-parallel pump- and probe- interactions, suggesting multiple orthogonal band 'valleys' created through Q_x and Q_y π- stacking interactions between adjacent stacked phthalocyanine chromophores within a single aggregate. Both 2DES pulse sequences reveal that this electronic structure is not substantially changed upon association with other aggregates through hydrogen bonding.

Fluence-dependent Pump-Probe Spectroscopy and Observation of Exciton Hopping

We performed fluence-dependent pump-probe spectroscopy on single aggregates and HOFs. We varied the pump fluence while maintaining a constant probe fluence to collect fluence-dependent spectra. Probe fluence was always less than 10% of pump fluence in all experiments. Typically, signal from higher-order processes, like biexciton formation, decays with the probe time delay because of EEA. Fluence-dependent pump-probe time traces from the excited-state absorption features up to 10 ps for single aggregates and HOFs are shown in Figs. 4a, b. In isolated aggregates, the signal follows a quadratic increase as a function of the laser fluence, indicating that a detectable fraction of the signal is from fifth order Feynman pathways[8,15,42–45], or second order kinetics of excitons. Although we observe a quadratic increase in pump-probe signal with pump fluence in single aggregates, we do not observe a change in the time-dependent exciton dynamics in single aggregates as a function of pump fluence. For single aggregates, we posit that the absence of fluence dependence is due to the coherent suppression of exciton-exciton annihilation[11,16,18] because at a fluence of 86 nJ per pulse, annihilation is observed in the HOF in 2 ps, and this timescale is in excellent agreement with the literature[22,23]. In our kinetic analysis, we use the pump-probe spectra at the earliest positive waiting time to first calculate the coherence size i.e., the number of monomers in a HOF across which the exciton is delocalized immediately after exciting with a pump pulse. We compute the coherence size of the HOF using the formalism described by Scherer and co-workers[46] to be 11 ± 3. This quantity is then used to compute the number of excitations per HOF absorbing unit for each pump fluence by following the method described by Dostal and co-workers[8], and we obtain values of 0.5, 0.7, 1.1, and 1.5 excitations per HOF absorbing unit for pump fluences of 27, 40, 62 and 86 nJ respectively. These calculations are detailed in Supplementary Notes Section 4.2. This is used in the integrated second order rate equation[10] to fit the PIA signal of the HOFs that yield time constants of 2–3 ps and the calculation is shown in Supplementary Notes Section 4.3. At the same fluence, signal in dispersed separated aggregates is clearly in the fifth-order regime (signal intensity increases quadratically with pump fluence, see Fig. 4b inset), but it does not show time-dependent second-order kinetics from annihilation. Singular value decomposition (SVD) of pump-probe data up to 10 ps suggests that there is only one principal component that captures almost all of the signal. This component reproduces the fluence dependence as a function of waiting time in HOF and its absence in separated aggregates as shown in Supplementary Notes Section 4.1. In Supplementary Fig. 39, we show that the signal is a quadratic function of fluence even at 5 ps and 10 ps in isolated aggregates, when annihilation in the HOF is complete. Figure 4a inset shows that biexcitons are formed at high fluences in the HOF sample as well. However, this signal becomes linear with fluence at a waiting time of 5 ps, as

https://doi.org/10.1038/s41467-024-52341-2

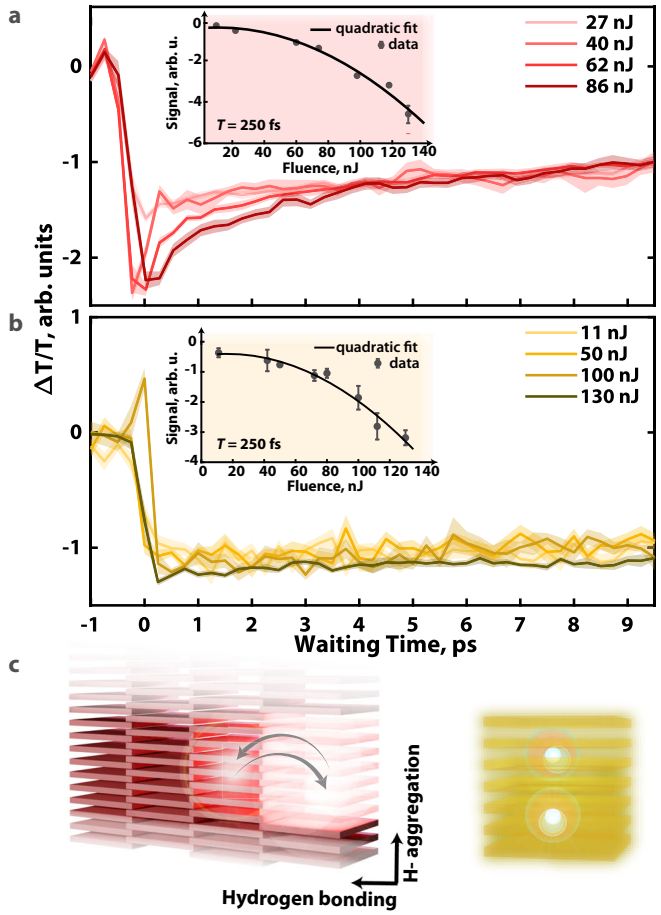

Fig. 4 | Fluence Dependent Pump-probe Spectroscopy of Single and Connected Aggregates. Dynamics of the pump-probe excited-state absorption feature at 580 nm are shown as a function of delay time for (**a**) connected aggregates (average of $n = 10$ replicates taken on the same sample for all fluences; shaded error bars are 1 standard error in the mean) all taken on the same sample for all fluences; shaded error bars are 1 standard error in the mean as are error bars on individual data points) and inset data for connected aggregates is collected separately: $n = 7$ replicates (10 nJ, 22 nJ), $n = 5$ replicates (60 nJ), $n = 7$ replicates (74 nJ), $n = 5$ replicates (98 nJ), $n = 7$ replicates (118 nJ), $n = 4$ replicates (130 nJ) (**b**) isolated aggregates (average of $n = 40$ replicates (11nJ), $n = 20$ replicates (42nJ), $n = 10$ replicates (72 nJ, 80 nJ), $n = 7$ replicates (100 nJ, 112 nJ), $n = 6$ replicates (130nJ). In the inset of **a** and **b**, the fluence dependence of the signal is shown. It is observed that the magnitude of the signal increases quadratically with pump-fluence, indicating the multi-exciton regime at higher fluences for both aggregate types. All traces are normalized to 10 ps. Source data for a and b are provided as a source data file. **c** A schematic showing the difference between connected and isolated aggregates' dynamics: in connected aggregates, exciton diffusion allows excitons of many different spatial phases to meet, whereas in isolated aggregates, the excitons remain on the same quantum site without annihilating.

shown in Supplementary Fig. 40, indicating negligible biexciton presence at this later waiting time, because annihilation induced by diffusion is complete. Moreover, a biexciton photoinduced absorption is clearly seen in the basic H-aggregate spectra at the earliest waiting times in 2DES. Two previous studies have reported the lack of EEA in H-aggregate excitons but reasonably attributed it to the inability of the aggregates to sustain multiexcitons at the time[19,47]. However, multiple works have now shown that in fact multiexcitons persist in H-aggregates with highly suppressed annihilation due to the oscillating H-like band structure[11,16,18]. Cross-peak specific 2DES spectra of single and connected aggregates have identical instantaneous signatures, demonstrating that multiple excitons can be formed along the same chromophores, but annihilation is not the only signature of their existence, as has been shown by Brixner and co-workers[11] and Huang and co-workers[16]. We conclude from the fluence-dependent spectra that the earlier reported timescales of exciton-exciton annihilation in H-aggregates are from hopping between distinct, weakly-coupled aggregates, but that within a single such aggregate, biexciton reservoirs can exist at room temperature without annihilating during the excited state lifetime.

When taken together, observations from 2DES and fluence-dependent pump-probe spectroscopy show that biexcitons can instantaneously form on isolated and connected H- aggregates upon interaction with pump or probe light, but that the formation of a biexciton is not sufficient to observe exciton-exciton annihilation. From 2DES, we argue that the biexciton is non-annihilating because the individual excitons within an aggregate are quantum mechanically non-interacting, possibly due to the orthogonal bands formed upon stacking of phthalocyanines, and due to the highly oscillatory spatial phases of the delocalized H- aggregate exciton wavefunction. Pump-probe experiments then confirm that if the non-interacting excitons in the single-aggregate, multi-exciton regime are allowed to diffuse, they lead to exciton-exciton annihilation due to increased sampling of spatial phases and valleys during exciton-exciton collisions.

Discussion

Negative coupling ($V_O < 0$) of molecular dipoles creates an excitonic manifold in which oscillator strength and brightness are redistributed to the lowest energy state, yielding redshifted absorption spectra of aggregates in comparison to monomers[12]. These aggregates are called J-aggregates. The spatial excitonic wavefunction of the bright state in J-aggregates is not oscillatory and the sum over all chromophore coefficients of the J-aggregate exciton wavefunction is high. Negative coupling is seen across pigments in many photosynthetic antennae[3,48,49] and effectively tunes absorption spectra for optimal performance in various ecological niches. Energy transport within synthetic J-aggregated structures has been demonstrated[28,50,51]. A drawback of utilizing J-aggregates for energy-harvesting applications is that the lowest energy exciton is optically bright, and fluorescence outcompetes exciton hopping if transport to the photoelectrode/reaction center is slow. Further, EEA is not suppressed in J- aggregates.

Positive coupling of dipoles creates an excitonic manifold in which the highest-energy exciton is bright, shifting the absorption spectra of these H-aggregates to bluer wavelengths with respect to their constituent chromophores[12]. The spatial wavefunction of the dark, lowest-energy state of H-aggregates is oscillatory. The rate of the EEA reaction is proportional to the square of the sum of wavefunction coefficients over the chromophores constituting the aggregate[18]. The alternating phase of the spatial wavefunction in H-aggregates reduces the sum of wavefunction coefficients over chromophore sites for different excitons so that they can remain on the same chromophores without interacting or annihilating[16,18]. Spatial properties of the delocalized wavefunction have been used in the past to govern reaction and tunneling rates[52,53]. The lowest energy exciton in the H-aggregate manifold is optically dark and energetic relaxation to this dark state is rapid[12]. The small transition dipole of the lowest excited state makes H-aggregates appealing for light-harvesting applications and several attempts have been made to design H-aggregated light-harvesting materials[18,54–59]. Trapping generally follows exciton localization in H-aggregated systems. Many traps are deep[35,56,60] and they prevent efficient exciton transport to the site of charge separation[6] as pointed by many studies[6,47,56,61,62]. Organic frameworks have potential as light harvesting antennae for their chromophore tunability[63], favorable FRET dipole alignment[64] and large exciton migration distances[6,65]. Here, we demonstrate long-range transport of excitons that remain delocalized, along a hydrogen-bonded organic framework.

Typically, H- aggregates of phthalocyanines and perylene-diimide families form with crystal structures in which exciton delocalization and

diffusion directions may not be orthogonal[22,23]. Such structures convolve dynamics originating from solely excited-state electronic structure and from exciton diffusion leading to multi-exciton events. The controlled self-assembly of the ZnOPPc and the orthogonal directions of delocalization and diffusion allows us to observe exciton dynamics without effects from exciton transfer between aggregates. Comparing exciton dynamics in linear aggregates and the HOF allows us to characterize exciton dynamics in H- aggregates as a sum of three effects: inherent excited state dynamics of single excitons, spontaneous biexciton formation on single aggregates with suppressed EEA, and exciton diffusion along the hydrogen-bonded arms of the framework.

In summary, we show that exciton-exciton collisions arising from exciton diffusion are required for exciton-exciton annihilation because collisions occur between excitons with different spatial phases. We show that when aggregates are isolated and exciton transfer between them is not possible, biexcitons can be formed through optical excitation on single quantum sites and can remain on the same site without annihilating. This finding suggests that H-aggregates may be able to create reservoirs of excitons to provide a steady flow of excitations to electrodes if exciton transfer between aggregates is prevented. From two-dimensional electronic spectroscopy, we see an instantaneous biexciton signature with negligible Rabi contraction, in agreement with the theory of Tempelaar and coworkers[18] where they suggest that the highly oscillating dark state wavefunction of H-aggregates makes the sum of wavefunction coefficients on individual sites (and thus coupling due to system-bath fluctuations) between distinct excitons minimal. Finally, using polarization-controlled 2DES, we show that phthalocyanine H-aggregate bands have orthogonal valleys that could be used as an optically addressable degree of freedom[66]. Our observations suggest that strongly coupled materials can perform the functions of a light harvesting antenna and an exciton reservoir at the same time[57].

Using a post-synthetic strategy of changing the pH of the aggregates' medium, we show a switch between annihilating and non-annihilating regimes using a chemical stimulus[67] at room temperature. This post-synthetic strategy allows us to access both states without significantly modifying the electronic structure of single aggregates and by directly controlling exciton diffusion rather than other properties that are frequently tuned to promote/hinder diffusion, like bandgap alignment[68] and defect placement[4]. The annihilating and non-annihilating regimes could be dynamically accessed with pH changes in future works akin to plant photoresponses that also rely on pH-dependent aggregation[69].

Methods

Sample Preparation

ZnOPPc powder was synthesized following the steps detailed in Suppl. Note 1. Dry DMSO (dimethyl sulfoxide) is added to the ZnOPPc powder. To make the aggregate solutions, a concentrated aliquot of ZnOPPc powder in dry DMSO is made. This is then diluted with deionized (DI) water (neutral pH by default) to make the framework of aggregate solution. The same aliquot is diluted with basic water (pH ~11 made by dissolving NaOH in DI water) to form the isolated aggregate solution. The samples were diluted with DMSO (for monomer) and pH-specific water (for the aggregates) until an optical density (OD) of less than 0.3 was reached in a 200 µm sample cell in order to avoid optical reabsorption events during nonlinear spectroscopy experiments.

Ultrafast Spectroscopy

Ultrafast measurements were carried out using sub-10 fs broadband pulses. A mode-locked oscillator (Coherent, Inc.) with a Ti:Sapphire crystal as the lasing medium operating at 80 MHz is used to seed a regenerative amplifier (Coherent, Inc.) which ultimately produces a pulse with a temporal FWHM of 40 fs and spectrally centered at 800 nm at a repetition rate of 5 kHz. This pulse propagates through a pressurized 2 m long Argon gas tube to create chirped broadband pulses in the visible regime with a bandwidth between 480 nm and 800 nm. Spectral filters (Thorlabs, Inc.) and chirped mirrors (Laser Quantum) are used to spectrally shape and temporally compress the pulse respectively. Beam-splitters (Thorlabs, Inc.) are used to create more than one pulse and optical translation stages (Aerotech, Inc.) are used to impart time-delays between pulses. Four pulses are created to perform two-dimensional electronic spectroscopy (2DES) experiments in the BOX-CARS geometry, and two pulses are created for pump-probe experiments. Half-waveplates (Thorlabs, Inc.) are used to control the relative linear polarization of the pulses for cross-peak specific 2DES measurements.

Data availability

All data supporting the findings of this study are detailed in the paper and the Supplementary Notes. The raw data generated in this study have been deposited in the FigShare database under accession code https://doi.org/10.6084/m9.figshare.26376118. The reduced data generated in this study are provided in the Supplementary Information/Source Data file. Source data are provided with this paper.

References

1. van Amerongen, H., van Grondelle, R. & Valkunas, L. *Photosynthetic Excitons*. (World Scientific, 2000).
2. Scholes, G. D., Fleming, G. R., Olaya-Castro, A. & van Grondelle, R. Lessons from nature about solar light harvesting. *Nat. Chem.* **3**, 763–774 (2011).
3. Brixner, T., Hildner, R., Köhler, J., Lambert, C. & Würthner, F. Exciton transport in molecular aggregates – from natural antennas to synthetic chromophore systems. *Adv. Energy Mater.* **7**, 1700236 (2017).
4. Delor, M., Weaver, H. L., Yu, Q. & Ginsberg, N. S. Imaging material functionality through three-dimensional nanoscale tracking of energy flow. *Nat. Mater.* **19**, 56–62 (2020).
5. Roy, P. et al. Ultrafast bridge planarization in donor-π-acceptor copolymers drives intramolecular charge transfer. *Nat. Commun.* **8**, 1–10 (2017).
6. Flanders, N. C. et al. Large exciton diffusion coefficients in two-dimensional covalent organic frameworks with different domain sizes revealed by ultrafast exciton dynamics. *J. Am. Chem. Soc.* **142**, 14957–14965 (2020).
7. Barzda, V. et al. Singlet–singlet annihilation kinetics in aggregates and trimers of LHCII. *Biophysical J.* **80**, 2409–2421 (2001).
8. Dostál, J. et al. Direct observation of exciton–exciton interactions. *Nat. Commun.* **9**, 2466 (2018).
9. Bittner, T., Irrgang, K.-D., Renger, G. & Wasielewski, M. R. Ultrafast excitation energy transfer and exciton-exciton annihilation processes in isolated light harvesting complexes of photosystem II (LHC II) from Spinach. *J. Phys. Chem.* **98**, 11821–11826 (1994).
10. Sun, D. et al. Observation of rapid exciton–exciton annihilation in monolayer molybdenum disulfide. *Nano Lett.* **14**, 5625–5629 (2014).
11. Malý, P. et al. Separating single- from multi-particle dynamics in nonlinear spectroscopy. *Nature* **616**, 280–287 (2023).
12. Hestand, N. J. & Spano, F. C. Expanded theory of H- and J-molecular aggregates: the effects of vibronic coupling and intermolecular charge transfer. *Chem. Rev.* **118**, 7069–7163 (2018).
13. Spano, F. C. The Spectral signatures of frenkel polarons in H- and J-aggregates. *Acc. Chem. Res.* **43**, 429–439 (2010).
14. Dahlberg, P. D. et al. Mapping the ultrafast flow of harvested solar energy in living photosynthetic cells. *Nat. Commun.* **8**, 988 (2017).
15. Lüttig, J., Mueller, S., Malý, P., Krich, J. J. & Brixner, T. Higher-Order Multidimensional and Pump–Probe Spectroscopies. *J. Phys. Chem. Lett.* **14**, 7556–7573 (2023).

16. Kumar, S. et al. Exciton annihilation in molecular aggregates suppressed through quantum interference. *Nature Chemistry* **15**, 1118–1126 (2023).
17. Navotnaya, P. et al. Annihilation of excess excitations along phycocyanin rods precedes downhill flow to allophycocyanin cores in the phycobilisome of synechococcus elongatus PCC 7942. *J. Phys. Chem. B* **126**, 23–29 (2022).
18. Tempelaar, R., Jansen, T. L. & Knoester, J. Exciton–exciton annihilation is coherently suppressed in H-Aggregates, but Not in J-aggregates. *J. Phys. Chem. Lett.* **8**, 6113–6117 (2017).
19. Mazuski, R. J. et al. Ultrafast excitation transfer in Cy5 DNA photonic wires displays dye conjugation and excitation energy dependency. *J. Phys. Chem. Lett.* **11**, 4163–4172 (2020).
20. Luo, T. et al. Nanoscale metal-organic framework confines zinc-phthalocyanine photosensitizers for enhanced photodynamic therapy. *J. Am. Chem. Soc.* **143**, 13519–13524 (2021).
21. Nash, G. T. et al. Nanoscale metal–organic layer isolates phthalocyanines for efficient mitochondria-targeted photodynamic therapy. *J. Am. Chem. Soc.* **143**, 2194–2199 (2021).
22. Kakade, S., Ghosh, R. & Palit, D. K. Excited state dynamics of zinc–phthalocyanine nanoaggregates in strong hydrogen bonding solvents. *J. Phys. Chem. C.* **116**, 15155–15166 (2012).
23. Li, X., Sinks, L. E., Rybtchinski, B. & Wasielewski, M. R. Ultrafast aggregate-to-aggregate energy transfer within self-assembled light-harvesting columns of zinc phthalocyanine tetrakis(perylenediimide). *J. Am. Chem. Soc.* **126**, 10810–10811 (2004).
24. Zanni, M. T., Ge, N.-H., Kim, Y. S. & Hochstrasser, R. M. Two-dimensional IR spectroscopy can be designed to eliminate the diagonal peaks and expose only the crosspeaks needed for structure determination. *Proc. Natl Acad. Sci.* **98**, 11265–11270 (2001).
25. Fidler, A. F., Singh, V. P., Long, P. D., Dahlberg, P. D. & Engel, G. S. Probing energy transfer events in the light harvesting complex 2 (LH2) of *Rhodobacter sphaeroides* with two-dimensional spectroscopy. *J. Chem. Phys.***139**, 155101 (2013).
26. Doria, S. et al. Understanding the influence of disorder on the exciton dynamics and energy transfer in Zn-phthalocyanine H-aggregates. *Phys. Chem. Chem. Phys.* **20**, 22331–22341 (2018).
27. Song, K.-H. et al. Quantum beats and phase shifts in two-dimensional electronic spectra of zinc naphthalocyanine monomer and aggregate. *J. Phys. Chem. Lett.* **6**, 4314–4318 (2015).
28. Wan, Y., Stradomska, A., Knoester, J. & Huang, L. Direct imaging of exciton transport in tubular porphyrin aggregates by ultrafast microscopy. *J. Am. Chem. Soc.* **139**, 7287–7293 (2017).
29. Fenn, E. E. & Fayer, M. D. Extracting 2D IR frequency-frequency correlation functions from two component systems. *J. Chem.Phys.* **135**, 074502 (2011).
30. Finkelstein-Shapiro, D. et al. Understanding radiative transitions and relaxation pathways in plexcitons. *Chem* **7**, 1092–1107 (2021).
31. Son, M. et al. Energy cascades in donor-acceptor exciton-polaritons observed by ultrafast two-dimensional white-light spectroscopy. *Nat. Commun.* **13**, 7305 (2022).
32. Wood, R. E. et al. Evidence for the dominance of carrier-induced band gap renormalization over biexciton formation in cryogenic ultrafast experiments on MoS_2 monolayers. *J. Phys. Chem. Lett.* **11**, 2658–2666 (2020).
33. Ramasesha, K., De Marco, L., Mandal, A. & Tokmakoff, A. Water vibrations have strongly mixed intra- and intermolecular character. *Nat. Chem.* **5**, 935–940 (2013).
34. Hamm, P. & Zanni, M. *Concepts and Methods of 2D Infrared Spectroscopy*. (Cambridge University Press, 2011).
35. Roy, P., Bressan, G., Gretton, J., Cammidge, A. N. & Meech, S. R. Ultrafast excimer formation and solvent controlled symmetry breaking charge separation in the excitonically coupled subphthalocyanine dimer. *Angew. Chem. Int. Ed.* **60**, 10568–10572 (2021).
36. Xiang, B. et al. Two-dimensional infrared spectroscopy of vibrational polaritons. *Proc. Natl Acad. Sci.* **115**, 4845–4850 (2018).
37. Dreyer, J., Moran, A. M. & Mukamel, S. Tensor components in three pulse vibrational echoes of a rigid dipeptide. *Bull. -Korean Chem. Soc.* **24**, 1091–1096 (2003).
38. Ricciardi, G., Rosa, A. & Baerends, E. J. Ground and excited states of zinc phthalocyanine studied by density functional methods. *J. Phys. Chem. A* **105**, 5242–5254 (2001).
39. Gutiérrez-Meza, E. et al. Frenkel biexcitons in hybrid HJ photophysical aggregates. *Sci. Adv.* **7**, eabi5197 (2021).
40. Chakrabarti, A. et al. Evidence for exciton-exciton binding in a molecular aggregate. *Phys. Rev. B* **57**, R4206–R4209 (1998).
41. Armstrong, Z. T. et al. Spatial heterogeneity of biexcitons in two-dimensional ruddlesden–popper lead iodide perovskites. *J. Am. Chem. Soc.* **145**, 18568–18577 (2023).
42. Zhang, Z., Lambrev, P. H., Wells, K. L., Garab, G. & Tan, H.-S. Direct Observation of multistep energy transfer in LHCII with fifth-order 3D electronic spectroscopy. *Nat. Commun.* **6**, 7914 (2015).
43. Lüttig, J., Brixner, T. & Malý, P. Anisotropy in fifth-order exciton–exciton-interaction two-dimensional spectroscopy. *J. Chem. Phys.* **154,** 154202 (2021).
44. Süß, J., Wehner, J., Dostál, J., Brixner, T. & Engel, V. Mapping of exciton–exciton annihilation in a molecular dimer via fifth-order femtosecond two-dimensional spectroscopy. *J. Chem. Phys.* **150**, 104304 (2019).
45. Rose, P. A. & Krich, J. J. Interpretations of high-order transient absorption spectroscopies. *J. Phys. Chem. Lett.* **14**, 10849–10855 (2023).
46. Book, L. D., Ostafin, A. E., Ponomarenko, N., Norris, J. R. & Scherer, N. F. Exciton delocalization and initial dephasing dynamics of purple bacterial LH2. *J. Phys. Chem. B* **104**, 8295–8307 (2000).
47. Kaufmann, C. et al. Ultrafast exciton delocalization, localization, and excimer formation dynamics in a highly defined perylene bisimide quadruple π-stack. *J. Am. Chem. Soc.* **140**, 4253–4258 (2018).
48. Sil, S. et al. Excitation energy transfer and vibronic coherence in intact phycobilisomes. *Nat. Chem.* **14**, 1286–1294 (2022).
49. Policht, V. R. et al. Hidden vibronic and excitonic structure and vibronic coherence transfer in the bacterial reaction center. *Sci. Adv.* **8**, eabk0953 (2022).
50. Zhu, T., Wan, Y. & Huang, L. Direct imaging of frenkel exciton transport by ultrafast microscopy. *Acc. Chem. Res.* **50**, 1725–1733 (2017).
51. Lin, H. et al. Collective fluorescence blinking in linear j-aggregates assisted by long-distance exciton migration. *Nano Lett.* **10**, 620–626 (2010).
52. Garner, M. H. et al. Comprehensive suppression of single-molecule conductance using destructive σ-interference. *Nature* **558**, 415–419 (2018).
53. Parenti, K. R. et al. Quantum interference effects elucidate triplet-pair formation dynamics in intramolecular singlet-fission molecules. *Nat. Chem.* **15**, 339–346 (2023).
54. Sung, J., Kim, P., Fimmel, B., Würthner, F. & Kim, D. Direct observation of ultrafast coherent exciton dynamics in helical π-stacks of self-assembled perylene bisimides. *Nat. Commun.* **6**, 8646 (2015).
55. Lim, J. M. et al. Exciton Delocalization and dynamics in helical π-stacks of self-assembled perylene bisimides. *Chem. Sci.* **4**, 388–397 (2013).
56. Samanta, S. et al. Safeguarding long-lived excitons from excimer traps in h-aggregated dye-assemblies. *Chem. Sci.* **11**, 5710–5715 (2020).
57. Haedler, A. T. et al. Long-range energy transport in single supramolecular nanofibres at room temperature. *Nature* **523**, 196–199 (2015).

58. Saikin, S. K. et al. On the long-range exciton transport in molecular systems: the application to h-aggregated heterotriangulene chains. *J. Phys. Chem. C.* **121**, 24994–25002 (2017).
59. Ahn, H. & Chu, T.-C. Annealing-induced phase transition in zinc phthalocyanine ultrathin films. *Opt. Mater. Express* **6**, 3586–3593 (2016).
60. Fink, R. F. et al. Exciton trapping in π-conjugated materials: a quantum-chemistry-based protocol applied to perylene bisimide dye aggregates. *J. Am. Chem. Soc.* **130**, 12858–12859 (2008).
61. Samanta, S. & Chaudhuri, D. Suppressing excimers in h-aggregates of perylene bisimide folda-dimer: role of dimer conformation and competing assembly pathways. *J. Phys. Chem. Lett.* **8**, 3427–3432 (2017).
62. Kramar, B. V. et al. Light harvesting antenna properties of framework solids. *Acc. Mater. Res.* **3**, 1149–1159 (2022).
63. Zhang, X., Geng, K., Jiang, D. & Scholes, G. D. Exciton diffusion and annihilation in an sp2 carbon-conjugated covalent organic framework. *J. Am. Chem. Soc.* **144**, 16423–16432 (2022).
64. Yu, J. et al. Improving energy transfer within metal–organic frameworks by aligning linker transition dipoles along the framework axis. *J. Am. Chem. Soc.* **142**, 11192–11202 (2020).
65. Zhang, Q. et al. Förster energy transport in metal–organic frameworks is beyond step-by-step hopping. *J. Am. Chem. Soc.* **138**, 5308–5315 (2016).
66. Lloyd, L. T. et al. Sub-10 fs intervalley exciton coupling in monolayer mos2 revealed by helicity-resolved two-dimensional electronic spectroscopy. *ACS Nano* **15**, 10253–10263 (2021).
67. Fresch, E. & Collini, E. The role of H-bonds in the excited-state properties of multichromophoric systems: static and dynamic aspects. *Molecules* **28**, 3553 (2023).
68. Chen, D., Nakahara, A., Wei, D., Nordlund, D. & Russell, T. P. P3HT/PCBM bulk heterojunction organic photovoltaics: correlating efficiency and morphology. *Nano Lett.* **11**, 561–567 (2011).
69. Son, M., Moya, R., Pinnola, A., Bassi, R. & Schlau-Cohen, G. S. Protein–protein interactions induce pH-dependent and zeaxanthin-independent photoprotection in the plant light-harvesting complex, LHCII. *J. Am. Chem. Soc.* **143**, 17577–17586 (2021).

Acknowledgements

This work made use of the shared facilities at the University of Chicago Materials Research Science and Engineering Center, supported by the National Science Foundation under award number DMR-2011854. This work made use of The University of Chicago Advanced Electron Microscopy Core Facility (RRID: SCR_019198). This work was made possible by financial support from the National Science Foundation through QuBBE QLCI (NSF OMA-2121044) through grant number 1900359 (received by GSE and used by SS, IG, CAJ, LTL, BCL, and GSE) and the Department of Energy through Award No. DE-SC0020131 (received by GSE and used by SS and GSE). SS thanks the Department of Chemistry, University of Chicago for the Benjamin Ball Freud Merit Scholarship for funding. Adobe Illustrator and Blender were used to render figures and graphics.

Author contributions

S.S., I.G., G.T.N., C.A.J., W.L. and G.S.E. conceived the research. G.T.N. performed monomer synthesis. S.S., I.G., G.T.N. and C.A.J. performed framework synthesis. I.G., S.S., C.A.J., L.T.L., B.C.L. performed nonlinear spectroscopy experiments. G.T.N., C.A.J., S.S., I.G., B.C.L., K.L.J. performed sample characterization. S.S., I.G., C.A.J. and G.S.E. performed data modeling. I.G., S.S., B.C.L. performed analysis of nonlinear spectroscopy data. Z.W. made the H.O.F. structural model. S.S., I.G., G.T.N. and G.S.E. wrote the paper. All authors provided feedback on writing. S.S. and I.G. contributed equally.

Competing interests

The authors declare no competing interests.

Additional information

Supplementary information The online version contains supplementary material available at https://doi.org/10.1038/s41467-024-52341-2.

Correspondence and requests for materials should be addressed to Gregory S. Engel.

Peer review information *Nature Communications* thanks the anonymous reviewers for their contribution to the peer review of this work. A peer review file is available.